Published in final edited form as:
Neuroimage. 2013 December ; 83: . doi:10.1016/j.neuroimage.2013.06.046.

Human occipital cortices differentially exert saccadic suppression: intracranial recording in children

Mitsugu Uematsu[1,5], **Naoyuki Matsuzaki**[1], **Erik C. Brown**[3,4], **Katsuaki Kojima**[1], and **Eishi Asano**[1,2,*]

[1]Department of Pediatrics, Wayne State University, Detroit, Michigan, 48201, USA

[2]Department of Neurology Children's Hospital of Michigan, Wayne State University, Detroit, Michigan, 48201, USA

[3]Psychiatry and Behavioral Neurosciences, Wayne State University, School of Medicine, Detroit, Michigan, 48201, USA

[4]MD-PhD Program, Wayne State University, School of Medicine, Detroit, Michigan, 48201, USA

[5]Department of Pediatrics Tohoku University, Graduate School of Medicine, Sendai, 980-8574, Japan

Abstract

By repeating saccades unconsciously, humans explore the surrounding world every day. Saccades inevitably move external visual images across the retina at high velocity; nonetheless, healthy humans don't perceive transient blurring of the visual scene during saccades. This perceptual stability is referred to as saccadic suppression. Functional suppression is believed to take place transiently in the visual systems, but it remains unknown how commonly or differentially the human occipital lobe activities are suppressed at the large-scale cortical network level. We determined the spatial-temporal dynamics of intracranially-recorded gamma activity at 80–150 Hz around spontaneous saccades under no-task conditions during wakefulness and those in darkness during REM sleep. Regardless of wakefulness or REM sleep, a small degree of attenuation of gamma activity was noted in the occipital regions during saccades, most extensively in the polar and least in the medial portions. Longer saccades were associated with more intense gamma-attenuation. Gamma-attenuation was subsequently followed by gamma-augmentation most extensively involving the medial and least involving the polar occipital region. Such gamma-augmentation was more intense during wakefulness and temporally locked to the offset of saccades. The polarities of initial peaks of perisaccadic event-related potentials (ERPs) were frequently positive in the medial and negative in the polar occipital regions. The present study, for the first time, provided the electrophysiological evidence that human occipital cortices differentially exert peri-saccadic modulation. Transiently suppressed sensitivity of the primary visual cortex in the polar region may be an important neural basis for saccadic suppression. Presence of occipital gamma-attenuation even during REM sleep suggests that saccadic suppression might be exerted even without external visual inputs. The primary visual cortex in the

*Corresponding Author: Eishi Asano, MD, PhD, MS (CRDSA), Address: Division of Pediatric Neurology, Children's Hospital of Michigan, Wayne State University. 3901 Beaubien St., Detroit, MI, 48201, USA. Phone: 313-745-5547; FAX: 313-745-0955; eishi@pet.wayne.edu.

medial region, compared to the polar region, may be more sensitive to an upcoming visual scene provided at the offset of each saccade.

Keywords

Intracranial recording; Electrocorticography (ECoG); High-frequency oscillations (HFOs); Ripples; Event-related potentials (ERPs); Corollary discharge; Efference copy signal

1. Introduction

Human vision remains stable despite the unstable visual input induced by saccades. This perceptual stability is referred to as saccadic suppression (Duffy and Lombroso, 1968), and functional suppression is believed to take place transiently in the visual systems (Burr et al., 1994). Studies of healthy humans using functional MRI (fMRI) and positron emission tomography (PET) failed to demonstrate consistent neural correlates of saccadic suppression; the occipital pole could be deactivated (Wenzel et al., 2000), unchanged (Kleiser et al., 2004) or even activated (Law et al., 1998; Sylvester et al., 2005) by saccades in darkness. Scalp EEG studies have not reported evidence of transient suppression of the human occipital activity during saccades (Forgacs et al., 2008). Studies of monkeys using microelectrode recording demonstrated transient reduction in firing rates, at the population level, in the superior colliculus (Ibbotson et al., 2008), lateral geniculate nucleus (Reppas et al., 2002; Saul, 2010), the primary visual cortex (V1) in the occipital lobe (Duffy and Burchfiel, 1975; Kagan et al., 2008; Rajkai et al., 2008), as well as portions of the temporal and parietal lobes (Ringo et al., 1994; Bremmer et al., 2009; Cloherty et al., 2010) around saccades. These microelectrode studies were designed to evaluate several neurons in a specific region of interest.

Here, we will delineate how commonly or differentially saccades modulate neural activities in distinct occipital regions at the large-scale cortical network level, using intracranially-recorded gamma activity at 80–150 Hz. Event-related augmentation of the amplitude of such gamma activity is generally considered to represent *in-situ* cortical activation (Crone et al., 2006). Sites showing event-related gamma-augmentation are associated with increased hemodynamic signals (Niessing et al., 2005; Scheeringa et al., 2011), increased firing rates (Ray et al., 2008), and relevant clinical symptoms resulting from cortical stimulation or resection (Kojima et al., 2012; Sinai et al., 2005). Conversely, a study of the occipital lobe of monkeys showed that sites showing event-related gamma-attenuation were associated with decreased hemodynamic signals and decreased firing rates (Shmuel et al., 2006). We sampled electrocorticography (ECoG) signals from the medial, inferior, lateral, and polar occipital regions (Matsuzaki et al., 2012) around spontaneous saccades associated with natural viewing during wakefulness and those in darkness during rapid eye movement (REM) sleep. This is a unique opportunity to simultaneously monitor neural activities in both superficial and deeply-situated human occipital cortices with millisecond scale temporal resolution and a spatial resolution of 1 cm. We chose to study REM sleep in darkness also, since the effects of saccade-induced changes in visual inputs can be minimized. We specifically hypothesized that gamma activity would be preferentially attenuated in the polar occipital region during saccades, because visual perception and awareness with a good spatial resolution are concentrated on objects presented in the central field (Levi et al., 1984). The polar occipital regions function as the primary visual cortex for the central field, according to the results of lesion (Horton and Hoyt, 1991), fMRI (Brewer et al., 2005) and electrophysiological studies (Rols et al., 2001; Yoshor et al., 2007). We also hypothesized that longer saccades would be associated with more intense occipital gamma-attenuation. Finally, we hypothesized that gamma activity would be augmented in

the occipital regions, following the offset of saccade when the fixed visual scene is newly provided. Testing the aforementioned hypotheses is expected to delineate the functional role of each occipital region in saccadic suppression.

2. Material and methods

2.1. Patients

We studied ten patients with focal epilepsy (age range: 5–17 years; 3 males, 7 females; Table 1) who satisfied the following inclusion and exclusion criteria. The inclusion criteria included: (i) extraoperative ECoG recording as a part of clinical management of medically-uncontrolled seizures at Children's Hospital of Michigan in Detroit, (ii) ECoG sampling from the occipital lobe, and (iii) availability of ECoG traces during wakefulness and REM sleep in the stored data files. The exclusion criteria included: (i) brain malformations involving the occipital lobe, (ii) oculomotor dysfunction or visual field defect detected by confrontation, and (iii) severe cognitive dysfunction reflected by verbal comprehension index of <70. All 10 patients had normal visual acuity. The study was approved by the Institutional Review Board at Wayne State University, and written informed consent was obtained from the guardians of all subjects.

2.2. Data acquisition

For ECoG recording, platinum grid and strip electrodes (10 mm intercontact distance, 4 mm diameter) were surgically implanted (Asano et al., 2009). Electrode placement involved all four lobes in one hemisphere, and the total number of analyzed electrodes ranged from 100 to 130 (mean: 108). All electrode plates were stitched to adjacent plates and/or the edge of dura mater, to avoid movement of subdural electrodes after placement. Intraoperative pictures were taken with a digital camera before dural closure. Planar x-ray images (lateral and anteroposterior) were subsequently acquired with the subdural electrodes in place for electrode localization on the brain surface (Dalal et al., 2008; Miller et al., 2007; Muzik et al., 2007); three metallic fiducial markers were placed at anatomically well-defined locations on the patient's head for co-registration of the x-ray image with the T1-weighted spoiled gradient echo MR image. A three-dimensional surface image was finally created with the location of electrodes directly defined on the brain surface (Alkonyi et al., 2009; Muzik et al., 2007; von Stockhausen et al., 1997). We confirmed the spatial accuracy of electrode display on the three-dimensional brain surface image, using intraoperative pictures (Dalal et al., 2008; Wellmer et al., 2002; Wu et al., 2011). By the age of 5 years, brain size becomes comparable to that of an adult (Dekaban and Sadowsky, 1978).

Based on the anatomical location (Kojima et al., in press; Matsuzaki et al., 2012; Mitelman et al., 2003; Nagasawa et al., 2011), each electrode site was classified into the following four categories (Table 2; Figures 1–3): (i) 'medial occipital region' defined as the medial portion of Brodmann Area (BA) 17/18 (N=47 sites in total); (ii) 'inferior occipital region' as the inferior portion of BA 19/37 (N=30 sites); (iii) 'lateral occipital region' as the lateral portion of BA 19/37 (N=42 sites); (iv) 'polar occipital region' as the polar portion of BA 17/18 (N=31 sites).

Extraoperative video-ECoG recordings were obtained using a 192-channel Nihon Kohden Neurofax 1100A Digital System (Nihon Kohden America Inc, Foothill Ranch, CA, USA). The sampling frequency was set at 1000 Hz with the amplifier band pass at 0.08–300 Hz. The averaged voltage of ECoG signals derived from the fifth and sixth intracranial electrodes of the ECoG amplifier was used as the original reference. ECoG signals were then re-montaged to a common average reference (Sinai et al., 2005; Wu et al., 2011). Channels contaminated with large interictal epileptiform discharges or artifacts were excluded from the common average reference. We have previously demonstrated that

saccade-related electromyography (EMG) artifacts on common average reference involved the anterior temporal but not the other regions (Nagasawa et al., 2011). No notch filter was used. All antiepileptic medications were discontinued on the day of subdural electrode placement. Electrodes overlying seizure onset zones were excluded from further analysis. Surface EMG electrodes were placed on the left and right deltoid muscles, and electrooculography (EOG) electrodes were placed 2.5 cm below and 2.5 cm lateral to the left and right outer canthi.

2.3. Marking of saccade events

No task was assigned to patients. Spontaneous saccades during natural viewing under room light as well as during REM sleep in darkness were marked as follows. REM sleep was determined with the help of video recording, according to the standard criteria (Bagshaw et al., 2009; Hori et al., 2001; Rechtschaffen and Kales, 1968). Complete darkness was not feasible since each patient was connected to several bio-monitoring systems placed outside the patient's visual field. Nonetheless, we assume that external visual inputs were minimal during REM sleep since the eyes were closed.

We marked each onset of saccade, defined as a rapid ocular movement reflected by an EOG amplitude change above 40 μV, with an angular departure of 45° or greater, and with a duration ranging from 40 to 200 ms (Hori et al., 2001; Qing and Kapoula, 2004; Rechtschaffen and Kales, 1968). Saccade events free from another saccade within ±1000 ms periods were included for further analysis (Table 2). We took this analytic approach to minimize the potential effect of another saccade on the amplitude of gamma activity around saccades of interest. Periods within two hours following seizures were excluded from analyses.

The duration of a saccade was defined as the period between the onset of signal rise and onset of signal fall on EOG with a time constant of 0.1 s. We determined the saccade duration of each marked event on each state in each patient. It has been previously reported that the amplitude of saccades is tightly correlated to the duration in healthy adults (Bahill et al., 1981) and that the peak velocities of saccades were 427±93 and 421±91 deg/s in healthy children and adults, respectively (Qing and Kapoula, 2004).

Saccades with smaller durations were not marked (as discussed in detail in the Discussion). Microsaccades are considered fixational eye movements, have durations generally ranging below 40 ms, and can be reliably detected using a high-frequency eye-tracker (Dimigen et al., 2009; Martinez-Conde et al., 2009; Yuval-Greenberg et al., 2008). We recognize that there are no universal criteria to clearly distinguish "gross/exploratory saccades" from "micro/fixational saccades", using the duration or amplitude. A feasible notion is that larger/longer saccades are likely to be of a more exploratory nature, whereas smaller/shorter ones more fixational (Martinez-Conde et al., 2004).

2.4. Measurement of saccade-related modulation of gamma activity

Each ECoG trial containing a saccade event was transformed into the time–frequency domain using a complex demodulation technique (Papp and Ktonas, 1977) incorporated in BESA® EEG V.5.1.8 software (BESA GmbH, Gräfelfing, German; Hoechstetter et al., 2004). The time–frequency transform was obtained by multiplication of the time-domain signal with a complex exponential, followed by a low-pass filter. The low-pass filter used here was a finite impulse response filter of Gaussian shape, making the complex demodulation effectively equivalent to a Gabor transform. The filter had a full width at half maximum of 2 × 7.9 ms in the temporal domain and 2 × 14.2 Hz in the frequency domain. The corresponding time-frequency resolution was ±7.9 ms and ±14.2 Hz (defined as the

50% power drop of the finite impulse response filter). A given ECoG signal was assigned an amplitude (a measure proportional to the square root of power) as a function of time and frequency at each trial. Time–frequency transformation was performed for frequencies between 20 and 300 Hz and latencies between −1000 and 1000 ms relative to the onset of saccades, in steps of 10 Hz and 5 ms. At each time-frequency bin, we analyzed the percent change in amplitude (averaged across trials) relative to the mean amplitude in a reference period between 300 and 100 ms prior to the saccade onset. Such a change in amplitude has been termed “temporal spectral evolution” (TSE) (Salmelin and Hari, 1994). In the present study of perisaccadic gamma-modulations, we did not differentiate between phase-locked and non-phase-locked components (Crone et al., 2006; Fukuda et al., 2008) of TSE values (Figure 4).

To test for statistical significance for each obtained TSE value, the following statistics were performed using BESA software (Kojima et al., 2012; Wu et al., 2011). First, a studentized bootstrap statistics was applied to obtain an uncorrected p-value independently for each time-frequency bin. This test compared the amplitude in each time-frequency bin with the averaged amplitude in the reference time period of the corresponding frequency. In a second step, correction for multiple testing was performed on these uncorrected p-values, accounting for the fact that TSE values at neighboring time bins are partially dependent. For that purpose, a modification of the Bonferroni correction developed by Simes (Simes, 1986) was used: for each channel and each frequency, p-values were sorted in ascending order (p_i, i=1, …, N, where N is the number of time bins in a given frequency band). The maximum index m in the sorted array for which $p_I < \alpha \cdot i/N$ was determined. All TSE values with $i < m$ were considered statistically significant. The corrected significance level α was set to 0.05.

We calculated the proportion of sites showing significant amplitude modulation spanning at least 20-Hz in width and at least 20-msec in duration among all sites in each occipital region in each patient (Figure 5). Such correction provides a very small probability of Type-I error in determination of cortical activation or deactivation. We recognize that this analysis may potentially underestimate gamma-modulations with a restricted frequency band (less than 20 Hz in width) or those with very short durations (less than 20 ms). Some previous studies using scalp EEG recording showed augmentation of a narrow-range gamma-band oscillations around 40 Hz (Tallon-Baudry et al., 1996), whereas event-related gamma-modulations observed in intracranial ECoG studies commonly involved frequency bands ranging at least 20 Hz in width (Tallon-Baudry et al., 2005; Lachaux et al., 2006; Nagasawa et al., 2011). We previously reported that electrical stimulation of sites showing gamma-augmentation with such spanning in width and duration resulted in relevant sensory, motor, and language symptoms with statistically-significant accuracy (Kojima et al., 2012; Nagasawa et al., 2010a; Nagasawa et al., 2010b). This procedure is expected to delineate how commonly across occipital regions and across patients saccade-related gamma-modulations took place during wakefulness and REM sleep (Figure 5).

2.5. Assessment of the temporal order of gamma-modulations

We determined the grand average of ‘gamma-amplitudes$_{80–150Hz}$’ across electrodes in each occipital region (Figure 6); thereby, ‘gamma-amplitude$_{80–150Hz}$’ reflects the percent-change of amplitude at 80–150 Hz compared to that in the reference period between 300 and 100 ms prior to the saccade onset. We believe this is a reasonable summary measure of *in-situ* occipital activity, since our previous study of the effect of photic stimulation in the occipital lobe revealed that the earliest and largest amplitude augmentation involved the 80–150 Hz frequency band (Matsuzaki et al., 2012). The peak frequency of gamma modulations during various forms of sensorimotor and cognitive tasks also involved this frequency band (Lachaux et al., 2006; Jerbi et al. 2010; Nagasawa et al., 2011; Ossandon et al. 2011; Kojima et al., in press). We determined when the grand average of gamma-amplitudes$_{80–150Hz}$ at

each occipital region differed from zero, using a one-sample Wilcoxon signed rank test (Figure 6).

2.6. Comparison of the magnitude of gamma-modulations across regions and states

Using the statistical software incorporated in JMP Pro Version 9.0.2. (SAS Institute Inc., Cary, NC, USA), we subsequently determined whether the least square (LS) means of minimum and maximum of gamma-amplitude$_{80–150Hz}$ differed among four occipital regions as well as across states (i.e.: wakefulness and REM sleep). This analysis was done using a mixed-model ANOVA, with regions and states treated as fixed effects and patients treated as a random effect; thereby, the REML method (restricted or residual maximum likelihood method) solved the ANOVA models with random effects (Biernaskie and Gegear, 2007; Qazi et al., 2003). If the ANOVA revealed that the p-value was less than 0.05, the Tukey's honestly significant difference (HSD) post-hoc test was applied to compare the LS means of gamma-amplitude$_{80–150Hz}$ between each pair of occipital regions.

2.7. Correlation between the saccade duration and the degree of gamma-attenuation

We determined whether longer saccades were associated with more intense gamma-attenuation. At each occipital site in each patient, we determined the regression slope of the minimum gamma-amplitude$_{80–150Hz}$ as a function of the duration of a given saccade event. We determined, at each state, whether the median regression slope differed from zero, using a one-sample Wilcoxon signed rank test.

2.8. Assessment of event-related potentials (ERPs)

We averaged ECoG traces, during wakefulness, time-locked to the saccade onset and offset, and computed event-related potentials (Purpura et al., 2003), the secondary measures of interest in the present study (Figure 3). We subsequently measured the baseline-to-peak voltage and latency of the initial ERP peak. We determined if the LS means of "baseline-to-peak voltage" and "latency" differed among four occipital regions as well as across analytic methods (i.e.: time-locking to the saccade onset versus that to the offset), as performed above.

3. Results

3.1. Behavioral results

A total of 591 saccades during wakefulness and 265 during REM sleep were marked (Table 2). The mean duration of saccades was 83.9 ms (median: 79 ms; standard deviation [SD]: 23.3 ms) during wakefulness, and 99.4 ms (median: 95 ms; SD: 28.3 ms) during REM sleep. The saccade duration during REM sleep was significantly longer than that during wakefulness ($p<0.05$ on Mann–Whitney U test), though the effect size was small.

3.2. Spatial-temporal characteristics of saccade-related gamma-modulations

Analysis, at the individual electrode level, revealed that significant gamma-attenuation was noted in 36% (54/150) of the entire occipital sites during saccades in wakefulness (Figure 5; Table S1) and in 6.7% (10/150) during REM sleep. The observation of a smaller proportion of occipital sites showing significant gamma-attenuation is partially attributed to the smaller number of saccade events during REM sleep (Table 2). Saccade-related gamma-attenuation involved the polar occipital region most extensively (Figures 2–5) and earliest among the four regions (Figure 6). Gamma-attenuation least extensively involved the medial occipital region. The present study failed to find gamma-attenuation in the regions other than the four occipital regions.

Gamma-augmentation subsequently involved the medial occipital region most extensively (Figure 5) and earliest among the four regions (Figure 6). Such gamma-augmentation was more prominent during wakefulness compared to during REM sleep (Figure 6). Further analysis revealed a gradient in gamma-modulation profiles across neighboring sites; medial-occipital gamma-augmentation was more intensive in the anterior portion compared to the posterior portion (Figure 7). Trial-by-trial analysis revealed that medial-occipital gamma-augmentation was better time-locked to the saccade offset than the onset (Figure 8). These observations indicate that medial-occipital gamma-augmentation was elicited by a new visual scene provided at the offset of each saccade. The present study failed to find gamma-augmentation of cortical origin in extra-occipital regions before or after the saccades.

Group analysis of saccade-related gamma-attenuation using a mixed-model ANOVA revealed a significant effect of regions on the LS means of minimum gamma-amplitude$_{80–150Hz}$ ($F=4.19$; $p=0.006$), while neither effect of states ($F=2.59$; $p=0.11$) nor interaction between regions and states ($F=0.38$; $p=0.77$) were found. The Tukey's HSD test confirmed that the LS means of minimum gamma-amplitude$_{80–150Hz}$ was smaller in the polar compared to the medial occipital region during saccades ($p=0.004$); in other words, gamma-attenuation following the onset of saccades was more intense in the polar compared to the medial occipital region.

Likewise, the analysis of gamma-augmentation revealed a significant effect of regions ($F=41.72$; $p<0.0001$) and states (wakefulness > REM sleep; $F=22.97$; $p<0.0001$) on the LS means of maximum gamma-amplitude$_{80–150Hz}$; no significant interaction between regions and states was found ($F=0.80$; $p=0.50$). The Tukey's HSD test confirmed that the LS means of maximum gamma-amplitude$_{80–150Hz}$ was larger in the medial compared to the polar, lateral and inferior occipital regions ($p<0.0001$; $p<0.0001$; $p<0.0001$, respectively), and larger in the inferior compared to the polar and lateral regions ($p=0.0006$ and $p=0.02$, respectively). In short, gamma-augmentation was most intense in the medial, second most intense in the inferior, and least intense in the polar occipital region; in addition, wakefulness increased the degree of overall occipital gamma-augmentation.

3.3. Correlation between the saccade duration and gamma-attenuation

Figure 9 presents the temporal changes of gamma-amplitudes$_{80–150Hz}$, during wakefulness, averaged across all occipital sites in two groups: (i) the group with saccade trials with durations shorter than the median of each patient and (ii) the other group with trials with longer saccade durations. Longer saccades, compared to shorter ones, were associated with more intense perisaccadic gamma-attenuation (Figure 9). The one-sample Wilcoxon signed rank test also demonstrated that the median regression slope (across all occipital sites) of the minimum gamma-amplitude$_{80–150Hz}$ as a function of the duration of a given saccade was below zero during wakefulness ($p=0.0024$) as well as during REM sleep ($p<0.0001$).

3.4. Spatial-temporal characteristics of event-related potentials (ERPs)

Visual assessment of ERPs time-locked to the saccade onset and offset suggested that the polarity of first perisaccadic ERP peak was often positive in the medial occipital region and negative in the polar and lateral occipital regions (Figures 3 and 10). Group analysis of ERPs using a mixed-model ANOVA revealed a significant effect of regions on the LS means of baseline-to-peak voltage ($F=42.7$; $p<0.001$), while neither effect of analytic methods ($F=0.13$; $p=0.72$) nor interaction between regions and analytic methods ($F=0.05$; $p=0.98$) was found. The Tukey's HSD test confirmed that the LS means of baseline-to-peak voltage was more positive in the medial compared to in the polar, lateral, and inferior occipital regions ($p<0.001$) and also more positive in the inferior compared to in the polar occipital region ($p=0.005$).

Analysis of the latency of the first perisaccadic ERP peak revealed a significant effect of regions ($F=6.59$; $p<0.001$) and analytic methods ('time-locked to the saccade onset' versus 'time-locked to the offset'; $F=236.8$; $p<0.001$) on the LS means of peak latency, while no interaction between regions and analytic methods ($F=1.58$; $p=0.19$) was found. The Tukey's HSD test confirmed that the LS means of peak latency was shorter in the medial compared to in the polar ($p=0.005$), lateral ($p=0.004$), and inferior occipital regions ($p=0.001$).

4. Discussion

4.1. Significance of saccade-related gamma-modulations in the occipital lobe

The present study, for the first time, provided the electrophysiological evidence that human occipital cortices differentially exert saccadic suppression. Statistical analysis, at the regional level, revealed that the amplitude of gamma activity at 80–150 Hz began to be reduced at the saccade onset, most intensely in the polar occipital region and least in the medial occipital region (Figure 5). The temporal profiles of perisaccadic modulations of gamma amplitudes in the medial occipital region (Figure 6) were similar to those of neuronal firing at a portion of V1 in monkeys (Kagan et al., 2008). The latency and duration of occipital gamma-attenuation coincide with those of perceptual saccadic suppression described in previous behavioral studies (Bruno et al., 2006; Volkmann et al., 1968). Saccade-related gamma-attenuation in the polar and lateral occipital regions lingered even after the offset of saccades (Figure 6). The occipital pole in human brain serves as the primary visual cortex for the central field (Brewer et al., 2005; Rols et al., 2001; Ruff et al., 2006; Yoshor et al., 2007). Lesions involving the occipital poles resulted in central visual field defects, while those involving the medial surface of the occipital lobes resulted in peripheral defects (Horton and Hoyt, 1991; Spalding, 1952; Teuber et al., 1960). Electrical stimulation of the occipital pole consistently induces perception of simple forms of transient light (i.e.: phosphenes) in the more central field, whereas that of the more anterior-medial portion of the occipital lobe induces ones in the more peripheral field (Asano et al., 2009; Brindley and Lewin, 1968). A behavioral study showed that the effect of saccadic suppression was stronger in the central visual field than in more peripheral one (Bridgeman and Fisher, 1990). Transient suppression of early processing with a good spatial resolution in the central visual field may be an important neural basis for saccadic suppression.

Saccade-related gamma-attenuation was noted, to a comparable degree, during wakefulness under room light and REM sleep in darkness. Thus, it was difficult to explain saccade-related gamma-attenuation simply by the sudden changes in external visual inputs alone. Our observations rather support 'the corollary discharge/efference copy theory' that the motor systems generate a motor command signal to move the eyes and a copy signal to the visual systems (Sperry, 1950; Zaretsky and Rowell, 1979). It has been hypothesized that the superior colliculus, medial dorsal nucleus of the thalamus, and frontal/supplementary/parietal eye fields might serve as the corollary discharge pathway (Schlag and Schlag-Rey, 2002; Ibbotson et al., 2008; Sommer and Wurtz, 2008). Several ECoG studies have reported that the frontal, supplementary, and parietal eye fields showed gamma-augmentation immediately preceding the onset of saccades (Lachaux et al., 2006; Nagasawa et al., 2011). The present study failed to find saccade-related gamma-modulations in the extra-occipital regions. A study of monkeys using microelectrode recording reported that firing rates were transiently reduced in the medial superior temporal region around saccades in the absence of visual stimuli (Bremmer et al., 2009), while such reduction in the middle temporal, ventral intra-parietal or lateral intra-parietal regions was associated with the presence of visual stimuli. The medial superior temporal region was not sampled in the present study utilizing subdural disk electrodes. We still do not know whether saccade-related gamma-attenuation in the occipital regions takes place via mechanisms similar to those which induce task-related gamma-attenuation in default-mode network areas such as the medial parietal and

prefrontal regions (Miller et al., 2009; Jerbi et al., 2010; Ossandón et al., 2011). Further human studies using intracranial disk and depth electrodes are warranted to localize the corollary discharge pathway by finding the cortical site at which stimulation alters saccade-related gamma-modulations and performance on a task that depends on saccadic suppression.

Saccade-related gamma-augmentation was noted most extensively in the medial-occipital region, more intense during wakefulness, and better time-locked to the offset of saccades. Thus, it is likely that such gamma-augmentation partly reflects the early visual processing of fixed visual scenes provided at the offset of each saccade. Smaller but still significant saccade-related gamma-augmentation was noted in the medial and inferior occipital regions even during REM sleep in the present study, as similarly reported in a scalp EEG study conducted in complete darkness during wakefulness (Forgacs et al., 2008). A feasible explanation for these observations is that scanning of the internal visual imagery might elicit such occipital gamma-augmentation. A behavioral study of patients with REM sleep behavior disorder suggested that REM imitates the scanning of the dream scene (Leclair-Visonneau et al., 2010).

4.2. Significance of perisaccadic ERPs in the occipital lobe

As best presented in Figure 3, perisaccadic ERPs were noted in both medial and polar occipital sites. Such ERPs were reflected as amplitude augmentation at low-frequency band on time-frequency plots and were accompanied by either augmentation or attenuation of gamma activity at 80–150 Hz. Thus, it was difficult to uni-directionally infer perisaccadic ERPs to be a neural marker of excitatory or inhibitory activity. A previous study of two epileptic patients using intracranial depth electrodes demonstrated the co-occurrence of ‘gamma-augmentation at >50 Hz’ and ‘positively-deflecting ERPs at <25 Hz’ in a medial occipital site immediately following the saccade offset during free viewing (Jerbi et al., 2009b). Studies using depth or disk electrodes likewise demonstrated the co-occurrence of ‘gamma-augmentation at >50 Hz’ and ‘positively- or negatively-deflecting ERPs at <25 Hz’ in the widespread occipital regions about 150 to 500 ms after visual presentation of an object (Vidal et al., 2010; Privman et al., 2011); thereby, the neural responses in the occipital pole were scarcely described due to the under-sampling. The novel observations in the present study include co-occurrence of gamma-attenuation and ERPs most commonly involving the polar occipital regions (Figures 3 and 10). We still don’t know the mechanism generating perisaccadic ERPs of opposite polarity with positivity in the medial and negativity in the polar occipital surfaces. Previous studies of somatosensory-evoked potentials (SSEPs) using intracranial subdural and depth electrodes demonstrated that the polarity of SSEPs at 20 ms was reversed across the central sulcus (Lueders et al., 1983; Allison et al., 1989; Szurhaj et al., 2006; Fukuda et al., 2008), while somatosensory-related gamma-augmentation emerged from the postcentral gyrus (Fukuda et al., 2008). Although SSEPs with variable polarity can be recorded in both postcentral and precentral gyri, it has been generally accepted that the main generator of SSEPs is localized to the anterior bank of postcentral gyrus (BA 3b) facing the central sulcus (Lueders et al., 1983; Allison et al., 1989). Further studies are warranted to determine whether variance in the polarity of perisaccadic ERPs across occipital regions can be explained by the mechanism generating the polarity reversal of SSEPs across the central sulcus.

4.3. Methodological issues

The present study revealed that saccade-related gamma-modulation profiles significantly differed across the four occipital regions. This observation does not indicate that each demarcated region plays a distinct role in saccadic suppression. As best presented in Figure 5, gamma-modulation profiles were similar across the polar and lateral occipital regions and

across the medial and inferior occipital regions. It has been suggested that the dorsal visual stream involving the lateral occipital region plays a role in the processing of location information, whereas the ventral visual stream involving the inferior occipital region plays an essential role in object recognition (Goodale and Milner, 1992; Mishkin and Ungerleider, 1982). As best presented in Figure 7, gamma-modulation profiles in medial occipital sites were gradually changed by the proximity of the polar region. We interpret our observations as suggesting that there is a gradient of the functional roles in saccadic suppression across occipital sites and that transient suppression of processing in larger proportions of the polar and lateral occipital neural populations and smaller proportions of the medial and inferior populations takes place during saccades.

Inherent limitations of studies using intracranial recording include sampling limitations. The locations of electrode placement were clinically determined, and were limited in occipital regions due to the presence of bridging veins. Depth electrodes were not utilized in our study population. It is quite possible that sampling errors contributed to failure to find an extra-occipital site showing significant perisaccadic gamma-augmentation in the present study. Significant perisaccadic gamma-augmentation in the frontal and parietal eye fields was reported in previous studies using depth (Lachaux et al., 2006) and disk electrodes (Nagasawa et al., 2011), where all patients were assigned specific tasks demanding attentive saccades toward a visual target. Conversely, spontaneous saccades under no-task conditions were analyzed in the present study. Failure to find extra-occipital gamma-augmentation could be partly attributed to the difference in experimental design. All patients were on various antiepileptic drugs, and the chronic effects of such medications on occipital gamma-modulations remains unknown (Zijlmans et al., 2009). The seizure onset zone and structural lesions were excluded from the analysis, in order to minimize their potential effects on saccade-related gamma-modulations (Jacobs et al., 2009; Kojima et al., 2012).

Reported saccade-related gamma-modulations could not be attributed to the effects of ocular EMG artifacts (Yuval-Greenberg et al., 2008; Worrell et al., 2012). Such EMG artifacts have been reported to increase the amplitude of gamma-activity in the anterior temporal region exactly at the onset of saccades (Jerbi et al., 2009a; Kovach et al., 2011; Nagasawa et al., 2011; Figure 11). In the present study, we found that the amplitude of occipital gamma-activity at 80–150 Hz was reduced at the onset of saccades and that the amplitude of such gamma-activity was increased following the offset of saccades.

In order to minimize the potential effects of a preceding event on ECoG signals, we have chosen saccades with an inter-saccade interval of at least 1,000 ms for the present study. The proportion of saccade events with such a long inter-saccade interval was larger in the present study of non-search-related eye movements under no-task conditions (Supplementary Figure S1), compared to in a previous study of saccades during a visual search task demanding close scrutiny (Dandekar et al., 2012). Another behavioral study reported that the rates of saccades were significantly smaller when subjects were assigned to freely view blank or natural scenes, compared to when they were assigned puzzling or searching tasks (Otero-Millan et al., 2008). We fully acknowledge that our selection criteria of saccade events resulted in a reduced number of analyzed events in each subject. Fortunately, direct recording of ECoG signals via subdural electrodes benefits from an excellent signal-to-noise ratio, which is 20 to above 100 times better than that of scalp EEG (Ball et al., 2009). Gamma-modulations and ERPs driven by single trials can be well visualized on intracranial recording (Vidal et al., 2010; Nagasawa et al., 2011; Lachaux et al., 2012). Moreover, each occipital region of interest had at least 30 electrode sites available for group analysis, which had a reasonable power to detect significant amplitude modulations and indeed demonstrated the novel spatial-temporal patterns of gamma-modulations and ERPs across occipital regions. Additional trial-by-trial suggested that perisaccadic gamma-attenuation in

the polar occipital region was noted regardless of the preceding inter-saccade interval (Supplementary Figure S1).

Reported saccade-related gamma-modulations are difficult to explain solely using the effects of unmarked microsaccades prior to the onset of gross saccades marked in the present study. Microsaccades are unconsciously exerted about 0.6 to 1.4 every second during natural viewing (Otero-Millan et al., 2008) and each microsaccade event elicits gamma-augmentation in the occipital region (Dimigen et al., 2009). Supposing that unmarked microsaccades preferentially have occurred during the reference period at 100 to 300 ms prior to the onset of marked saccades, our measurement of saccade-related gamma-modulations would have been greatly affected. Yet, there is no objective evidence that such preferential gamma-modulations occurred during the reference period (Figure 6; Supplementary Figure S1). Furthermore, significant correlation between saccade duration and the intensity of gamma-attenuation also suggests that observed gamma-attenuation was driven by the effect of a given saccade rather than that of preceding unmarked saccades (Figure 9).

Supplementary Material

Refer to Web version on PubMed Central for supplementary material.

Acknowledgments

We are grateful to Harry T. Chugani, MD, Sandeep Sood, MD, Robert Rothermel, PhD, Alanna Carlson, MA and the staff of the Division of Electroneurodiagnostics at Children's Hospital of Michigan, Wayne State University for the collaboration and assistance in performing the studies. This work was supported by NIH grants NS47550 and NS64033 (to E. Asano).

References

Alkonyi B, Juhasz C, Muzik O, Asano E, Saporta A, Shah A, Chugani HT. Quantitative brain surface mapping of an electrophysiologic/metabolic mismatch in human neocortical epilepsy. Epilepsy Res. 2009; 87:77–87. [PubMed: 19734012]

Allison T, McCarthy G, Wood CC, Darcey TM, Spencer DD, Williamson PD. Human cortical potentials evoked by stimulation of the median nerve. I. Cytoarchitectonic areas generating short-latency activity. J Neurophysiol. 1989; 62:694–710. [PubMed: 2769354]

Asano E, Juhasz C, Shah A, Sood S, Chugani HT. Role of subdural electrocorticography in prediction of long-term seizure outcome in epilepsy surgery. Brain. 2009; 132:1038–1047. [PubMed: 19286694]

Bagshaw AP, Jacobs J, LeVan P, Dubeau F, Gotman J. Effect of sleep stage on interictal high-frequency oscillations recorded from depth macroelectrodes in patients with focal epilepsy. Epilepsia. 2009; 50:617–628. [PubMed: 18801037]

Bahill AT, Brockenbrough A, Troost BT. Variability and development of a normative data base for saccadic eye movements. Invest Ophthalmol Vis Sci. 1981; 21:116–125. [PubMed: 7251295]

Ball T, Kern M, Mutschler I, Aertsen A, Schulze-Bonhage A. Signal quality of simultaneously recorded invasive and non-invasive EEG. Neuroimage. 2009; 46:708–716. [PubMed: 19264143]

Biernaskie JM, Gegear RJ. Habitat assessment ability of bumble-bees implies frequency-dependent selection on floral rewards and display size. Proc Biol Sci. 2007; 274:2595–2601. [PubMed: 17711839]

Bremmer F, Kubischik M, Hoffmann KP, Krekelberg B. Neural dynamics of saccadic suppression. J Neurosci. 2009; 29:12374–12383. [PubMed: 19812313]

Brewer AA, Liu J, Wade AR, Wandell BA. Visual field maps and stimulus selectivity in human ventral occipital cortex. Nat Neurosci. 2005; 8:1102–1109. [PubMed: 16025108]

Bridgeman B, Fisher B. Saccadic suppression of displacement is strongest in central vision. Perception. 1990; 19:103–111. [PubMed: 2336325]

Brindley GS, Lewin WS. The visual sensations produced by electrical stimulation of the medial occipital cortex. J Physiol. 1968; 194:54–55P. [PubMed: 5639368]

Bruno A, Brambati SM, Perani D, Morrone MC. Development of saccadic suppression in children. J Neurophysiol. 2006; 96:1011–1017. [PubMed: 16407425]

Burr DC, Morrone MC, Ross J. Selective suppression of the magnocellular visual pathway during saccadic eye movements. Nature. 1994; 371:511–513. [PubMed: 7935763]

Cloherty SL, Mustari MJ, Rosa MG, Ibbotson MR. Effects of saccades on visual processing in primate MSTd. Vision Res. 2010; 50:2683–2691. [PubMed: 20732345]

Crone NE, Sinai A, Korzeniewska A. High-frequency gamma oscillations and human brain mapping with electrocorticography. Prog Brain Res. 2006; 159:275–295. [PubMed: 17071238]

Dalal SS, Edwards E, Kirsch HE, Barbaro NM, Knight RT, Nagarajan SS. Localization of neurosurgically implanted electrodes via photograph-MRI-radiograph coregistration. J Neurosci Methods. 2008; 174:106–115. [PubMed: 18657573]

Dandekar S, Privitera C, Carney T, Klein SA. Neural saccadic response estimation during natural viewing. J Neurophysiol. 2012; 107:1776–1790. [PubMed: 22170971]

Dekaban AS, Sadowsky D. Changes in brain weights during the span of human life: relation of brain weights to body heights and body weights. Ann Neurol. 1978; 4:345–356. [PubMed: 727739]

Dimigen O, Valsecchi M, Sommer W, Kliegl R. Human microsaccade-related visual brain responses. J Neurosci. 2009; 29:12321–12331. [PubMed: 19793991]

Duffy FH, Burchfiel JL. Eye movement-related inhibition of primate visual neurons. Brain Res. 1975; 89:121–132. [PubMed: 807294]

Duffy FH, Lombroso CT. Electrophysiological evidence for visual suppression prior to the onset of a voluntary saccadic eye movement. Nature. 1968; 218:1074–1075. [PubMed: 5656628]

Forgacs PB, von Gizycki H, Selesnick I, Syed NA, Ebrahim K, Avitable M, Amassian V, Lytton W, Bodis-Wollner I. Perisaccadic parietal and occipital gamma power in light and in complete darkness. Perception. 2008; 37:419–432. [PubMed: 18491719]

Fukuda M, Nishida M, Juhász C, Muzik O, Sood S, Chugani HT, Asano E. Short-latency median-nerve somatosensory-evoked potentials and induced gamma-oscillations in humans. Brain. 2008; 131:1793–1805. [PubMed: 18508784]

Goodale MA, Milner AD. Separate visual pathways for perception and action. Trends Neurosci. 1992; 15:20–25. [PubMed: 1374953]

Hoechstetter K, Bornfleth H, Weckesser D, Ille N, Berg P, Scherg M. BESA source coherence: a new method to study cortical oscillatory coupling. Brain Topogr. 2004; 16:233–238. [PubMed: 15379219]

Hori T, Sugita Y, Koga E, Shirakawa S, Inoue K, Uchida S, Kuwahara H, Kousaka M, Kobayashi T, Tsuji Y, Terashima M, Fukuda K, Fukuda N. Proposed supplements and amendments to ‘A Manual of Standardized Terminology, Techniques and Scoring System for Sleep Stages of Human Subjects’, the Rechtschaffen & Kales (1968) standard. Psychiatry Clin Neurosci. 2001; 55:305–310. [PubMed: 11422885]

Horton JC, Hoyt WF. The representation of the visual field in human striate cortex. A revision of the classic Holmes map. Arch Ophthalmol. 1991; 109:816–824. [PubMed: 2043069]

Ibbotson MR, Crowder NA, Cloherty SL, Price NS, Mustari MJ. Saccadic modulation of neural responses: possible roles in saccadic suppression, enhancement, and time compression. J Neurosci. 2008; 28:10952–10960. [PubMed: 18945903]

Jacobs J, Levan P, Châtillon CE, Olivier A, Dubeau F, Gotman J. High frequency oscillations in intracranial EEGs mark epileptogenicity rather than lesion type. Brain. 2009; 132:1022–1037. [PubMed: 19297507]

Jerbi K, Freyermuth S, Dalal S, Kahane P, Bertrand O, Berthoz A, Lachaux JP. Saccade related gamma-band activity in intracerebral EEG: dissociating neural from ocular muscle activity. Brain Topogr. 2009a; 22:18–23. [PubMed: 19234780]

Jerbi K, Ossandón T, Hamamé CM, Senova S, Dalal SS, Jung J, Minotti L, Bertrand O, Berthoz A, Kahane P, Lachaux JP. Task-related gamma-band dynamics from an intracerebral perspective:

review and implications for surface EEG and MEG. Hum Brain Mapp. 2009b; 30:1758–1771. [PubMed: 19343801]

Jerbi K, Vidal JR, Ossandon T, Dalal SS, Jung J, Hoffmann D, Minotti L, Bertrand O, Kahane P, Lachaux JP. Exploring the electrophysiological correlates of the default-mode network with intracerebral EEG. Front Syst Neurosci. 2010; 4:27. [PubMed: 20661461]

Kagan I, Gur M, Snodderly DM. Saccades and drifts differentially modulate neuronal activity in V1: effects of retinal image motion, position, and extraretinal influences. J Vis. 2008; 8:19, 11–25. [PubMed: 19146320]

Kleiser R, Seitz RJ, Krekelberg B. Neural correlates of saccadic suppression in humans. Curr Biol. 2004; 14:386–390. [PubMed: 15028213]

Kojima K, Brown EC, Rothermel R, Carlson A, Fuerst D, Matsuzaki N, Shah A, Atkinson M, Basha M, Mittal S, Sood S, Asano E. Clinical significance and developmental changes of auditory-language-related gamma activity. Clin Neurophysiol. 201210.1016/j.clinph.2012.09.031

Kojima K, Brown EC, Rothermel R, Carlson A, Fuerst D, Matsuzaki N, Shah A, Mittal S, Sood S, Asano E. Gamma activity modulated by picture and auditory naming tasks: intracranial recording in patients with focal epilepsy. Clin Neurophysiol. in press.

Kovach CK, Tsuchiya N, Kawasaki H, Oya H, Howard MA 3rd, Adolphs R. Manifestation of ocular-muscle EMG contamination in human intracranial recordings. Neuroimage. 2011; 54:213–233. [PubMed: 20696256]

Lachaux JP, Axmacher N, Mormann F, Halgren E, Crone NE. High-frequency neural activity and human cognition: past, present and possible future of intracranial EEG research. Prog Neurobiol. 2012; 98:279–301. [PubMed: 22750156]

Lachaux JP, Hoffmann D, Minotti L, Berthoz A, Kahane P. Intracerebral dynamics of saccade generation in the human frontal eye field and supplementary eye field. Neuroimage. 2006; 30:1302–1312. [PubMed: 16412667]

Law I, Svarer C, Rostrup E, Paulson OB. Parieto-occipital cortex activation during self-generated eye movements in the dark. Brain. 1998; 121:2189–2200. [PubMed: 9827777]

Leclair-Visonneau L, Oudiette D, Gaymard B, Leu-Semenescu S, Arnulf I. Do the eyes scan dream images during rapid eye movement sleep? Evidence from the rapid eye movement sleep behaviour disorder model. Brain. 2010; 133:1737–1746. [PubMed: 20478849]

Levi DM, Klein SA, Aitsebaomo P. Detection and discrimination of the direction of motion in central and peripheral vision of normal and amblyopic observers. Vision Res. 1984; 24:789–800. [PubMed: 6474836]

Lueders H, Lesser RP, Hahn J, Dinner DS, Klem G. Cortical somatosensory evoked potentials in response to hand stimulation. J Neurosurg. 1983; 58:885–894. [PubMed: 6854381]

Martinez-Conde S, Macknik SL, Hubel DH. The role of fixational eye movements in visual perception. Nat Rev Neurosci. 2004; 5:229–240. [PubMed: 14976522]

Martinez-Conde S, Macknik SL, Troncoso XG, Hubel DH. Microsaccades: a neurophysiological analysis. Trends Neurosci. 2009; 32:463–475. [PubMed: 19716186]

Matsuzaki N, Nagasawa T, Juhász C, Sood S, Asano E. Independent predictors of neuronal adaptation in human primary visual cortex measured with high-gamma activity. Neuroimage. 2012; 59:1639–1646. [PubMed: 21945696]

Miller KJ, Makeig S, Hebb AO, Rao RP, denNijs M, Ojemann JG. Cortical electrode localization from X-rays and simple mapping for electrocorticographic research: The “Location on Cortex” (LOC) package for MATLAB. J Neurosci Methods. 2007; 162:303–308. [PubMed: 17343918]

Miller KJ, Weaver KE, Ojemann JG. Direct electrophysiological measurement of human default network areas. Proc Natl Acad Sci USA. 2009; 106:12174–12177. [PubMed: 19584247]

Mishkin M, Ungerleider LG. Contribution of striate inputs to the visuospatial functions of parieto-preoccipital cortex in monkeys. Behav Brain Res. 1982; 6:57–77. [PubMed: 7126325]

Mitelman SA, Shihabuddin L, Brickman AM, Hazlett EA, Buchsbaum MS. MRI assessment of gray and white matter distribution in Brodmann’s areas of the cortex in patients with schizophrenia with good and poor outcomes. Am J Psychiatry. 2003; 160:2154–2168. [PubMed: 14638586]

Muzik O, Chugani DC, Zou G, Hua J, Lu Y, Lu S, Asano E, Chugani HT. Multimodality data integration in epilepsy. Int J Biomed Imaging. 2007; 2007:13963. [PubMed: 17710251]

Nagasawa T, Matsuzaki N, Juhasz C, Hanazawa A, Shah A, Mittal S, Sood S, Asano E. Occipital gamma-oscillations modulated during eye movement tasks: simultaneous eye tracking and electrocorticography recording in epileptic patients. Neuroimage. 2011; 58:1101–1109. [PubMed: 21816225]

Nagasawa T, Rothermel R, Juhasz C, Fukuda M, Nishida M, Akiyama T, Sood S, Asano E. Cortical gamma-oscillations modulated by auditory-motor tasks-intracranial recording in patients with epilepsy. Hum Brain Mapp. 2010a; 31:1627–1642. [PubMed: 20143383]

Nagasawa T, Rothermel R, Juhasz C, Nishida M, Sood S, Asano E. Cortical gamma-oscillations modulated by visuomotor tasks: Intracranial recording in patients with epilepsy. Epilepsy Behav. 2010b; 18:254–261. [PubMed: 20580900]

Niessing J, Ebisch B, Schmidt KE, Niessing M, Singer W, Galuske RA. Hemodynamic signals correlate tightly with synchronized gamma oscillations. Science. 2005; 309:948–951. [PubMed: 16081740]

Ossandón T, Jerbi K, Vidal JR, Bayle DJ, Henaff MA, Jung J, Minotti L, Bertrand O, Kahane P, Lachaux JP. Transient suppression of broadband gamma power in the default-mode network is correlated with task complexity and subject performance. J Neurosci. 2011; 31:14521–14530. [PubMed: 21994368]

Otero-Millan J, Troncoso XG, Macknik SL, Serrano-Pedraza I, Martinez-Conde S. Saccades and microsaccades during visual fixation, exploration, and search: foundations for a common saccadic generator. J Vis. 2008; 8:21–18. [PubMed: 19146322]

Papp N, Ktonas P. Critical evaluation of complex demodulation techniques for the quantification of bioelectrical activity. Biomed Sci Instrum. 1977; 13:135–145. [PubMed: 871500]

Privman E, Fisch L, Neufeld MY, Kramer U, Kipervasser S, Andelman F, Yeshurun Y, Fried I, Malach R. Antagonistic relationship between gamma power and visual evoked potentials revealed in human visual cortex. Cereb Cortex. 2011; 21:616–624. [PubMed: 20624838]

Purpura KP, Kalik SF, Schiff ND. Analysis of perisaccadic field potentials in the occipitotemporal pathway during active vision. J Neurophysiol. 2003; 90:3455–3478. [PubMed: 12878708]

Qazi S, Samuel NK, Venkatachalam TK, Uckun FM. Evaluating dissolution profiles of an anti-HIV agent using ANOVA and non-linear regression models in JMP software. Int J Pharm. 2003; 252:27–39. [PubMed: 12550778]

Qing Y, Kapoula Z. Saccade-vergence dynamics and interaction in children and in adults. Exp Brain Res. 2004; 156:212–223. [PubMed: 15344851]

Rajkai C, Lakatos P, Chen CM, Pincze Z, Karmos G, Schroeder CE. Transient cortical excitation at the onset of visual fixation. Cereb Cortex. 2008; 18:200–209. [PubMed: 17494059]

Ray S, Crone NE, Niebur E, Franaszczuk PJ, Hsiao SS. Neural correlates of high-gamma oscillations (60–200 Hz) in macaque local field potentials and their potential implications in electrocorticography. J Neurosci. 2008; 28:11526–11536. [PubMed: 18987189]

Rechtschaffen, A.; Kales, A. A Manual of Standardized Terminology, Techniques and Scoring System for Sleep Stages of Human Subjects. Public Health Service. Government printing office; Washington DC: 1968.

Reppas JB, Usrey WM, Reid RC. Saccadic eye movements modulate visual responses in the lateral geniculate nucleus. Neuron. 2002; 35:961–974. [PubMed: 12372289]

Ringo JL, Sobotka S, Diltz MD, Bunce CM. Eye movements modulate activity in hippocampal, parahippocampal, and inferotemporal neurons. J Neurophysiol. 1994; 71:1285–1288. [PubMed: 8201422]

Rols G, Tallon-Baudry C, Girard P, Bertrand O, Bullier J. Cortical mapping of gamma oscillations in areas V1 and V4 of the macaque monkey. Vis Neurosci. 2001; 18:527–540. [PubMed: 11829299]

Ruff CC, Blankenburg F, Bjoertomt O, Bestmann S, Freeman E, Haynes JD, Rees G, Josephs O, Deichmann R, Driver J. Concurrent TMS-fMRI and psychophysics reveal frontal influences on human retinotopic visual cortex. Curr Biol. 2006; 16:1479–1488. [PubMed: 16890523]

Salmelin R, Hari R. Spatiotemporal characteristics of sensorimotor neuromagnetic rhythms related to thumb movement. Neuroscience. 1994; 60:537–550. [PubMed: 8072694]

Saul AB. Effects of fixational saccades on response timing in macaque lateral geniculate nucleus. Vis Neurosci. 2010; 27:171–181. [PubMed: 20932359]

Scheeringa R, Fries P, Petersson KM, Oostenveld R, Grothe I, Norris DG, Hagoort P, Bastiaansen MC. Neuronal dynamics underlying high- and low-frequency EEG oscillations contribute independently to the human BOLD signal. Neuron. 2011; 69:572–583. [PubMed: 21315266]

Schlag J, Schlag-Rey M. Through the eye, slowly: delays and localization errors in the visual system. Nat Rev Neurosci. 2002; 3:191–215. [PubMed: 11994751]

Shmuel A, Augath M, Oeltermann A, Logothetis NK. Negative functional MRI response correlates with decreases in neuronal activity in monkey visual area V1. Nat Neurosci. 2006; 9:569–577. [PubMed: 16547508]

Simes RJ. An improved Bonferroni procedure for multiple tests of significance. Biometrika. 1986; 73:751–754.

Sinai A, Bowers CW, Crainiceanu CM, Boatman D, Gordon B, Lesser RP, Lenz FA, Crone NE. Electrocorticographic high gamma activity versus electrical cortical stimulation mapping of naming. Brain. 2005; 128:1556–1570. [PubMed: 15817517]

Sommer MA, Wurtz RH. Brain circuits for the internal monitoring of movements. Annu Rev Neurosci. 2008; 31:317–338. [PubMed: 18558858]

Spalding JM. Wounds of the visual pathway. Part II. The striate cortex. J Neurol Neurosurg Psychiatry. 1952; 15:169–183. [PubMed: 14955691]

Sperry RW. Neural basis of the spontaneous optokinetic response produced by visual inversion. J Comp Physiol Psychol. 1950; 43:482–489. [PubMed: 14794830]

Sylvester R, Haynes JD, Rees G. Saccades differentially modulate human LGN and V1 responses in the presence and absence of visual stimulation. Curr Biol. 2005; 15:37–41. [PubMed: 15649362]

Szurhaj W, Labyt E, Bourriez JL, Kahane P, Chauvel P, Mauguière F, Derambure P. Relationship between intracerebral gamma oscillations and slow potentials in the human sensorimotor cortex. Eur J Neurosci. 2006; 24:947–954. [PubMed: 16930422]

Tallon-Baudry C, Bertrand O, Delpuech C, Pernier J. Stimulus specificity of phase-locked and non-phase-locked 40 Hz visual responses in human. J Neurosci. 1996; 16:4240–4249. [PubMed: 8753885]

Tallon-Baudry C, Bertrand O, Hénaff MA, Isnard J, Fischer C. Attention modulates gamma-band oscillations differently in the human lateral occipital cortex and fusiform gyrus. Cereb Cortex. 2005; 15:654–662. [PubMed: 15371290]

Teuber, HL.; Battersby, WS.; Bender, MB. Visual field defects after penetrating missile wounds of the brain. Harvard University Press; Cambridge, MA: 1960.

Vidal JR, Ossandón T, Jerbi K, Dalal SS, Minotti L, Ryvlin P, Kahane P, Lachaux JP. Category-Specific Visual Responses: An Intracranial Study Comparing Gamma, Beta, Alpha, and ERP Response Selectivity. Front Hum Neurosci. 2010; 4:195. [PubMed: 21267419]

Volkmann FC, Schick AM, Riggs LA. Time course of visual inhibition during voluntary saccades. J Opt Soc Am. 1968; 58:562–569. [PubMed: 5641658]

von Stockhausen H, Thiel A, Herholz K, Pietrzyk U. A convenient method for topographical localization of intracranial electrodes with MRI and a conventional radiograph. Neuroimage. 1997; 5:S514.

Wellmer J, von Oertzen J, Schaller C, Urbach H, Konig R, Widman G, Van Roost D, Elger CE. Digital photography and 3D MRI-based multimodal imaging for individualized planning of resective neocortical epilepsy surgery. Epilepsia. 2002; 43:1543–1550. [PubMed: 12460257]

Wenzel R, Wobst P, Heekeren HH, Kwong KK, Brandt SA, Kohl M, Obrig H, Dirnagl U, Villringer A. Saccadic suppression induces focal hypooxygenation in the occipital cortex. J Cereb Blood Flow Metab. 2000; 20:1103–1110. [PubMed: 10908044]

Worrell GA, Jerbi K, Kobayashi K, Lina JM, Zelmann R, Le Van Quyen M. Recording and analysis techniques for high-frequency oscillations. Prog Neurobiol. 2012; 98:265–78. [PubMed: 22420981]

Wu HC, Nagasawa T, Brown EC, Juhasz C, Rothermel R, Hoechstetter K, Shah A, Mittal S, Fuerst D, Sood S, Asano E. gamma-oscillations modulated by picture naming and word reading: intracranial recording in epileptic patients. Clin Neurophysiol. 2011; 122:1929–1942. [PubMed: 21498109]

Yoshor D, Bosking WH, Ghose GM, Maunsell JH. Receptive fields in human visual cortex mapped with surface electrodes. Cereb Cortex. 2007; 17:2293–2302. [PubMed: 17172632]

Yuval-Greenberg S, Tomer O, Keren AS, Nelken I, Deouell LY. Transient induced gamma-band response in EEG as a manifestation of miniature saccades. Neuron. 2008; 58:429–441. [PubMed: 18466752]

Zaretsky M, Rowell CH. Saccadic suppression by corollary discharge in the locust. Nature. 1979; 280:583–585. [PubMed: 460439]

Zijlmans M, Jacobs J, Zelmann R, Dubeau F, Gotman J. High-frequency oscillations mirror disease activity in patients with epilepsy. Neurology. 2009; 72:979–986. [PubMed: 19289737]

HIGHLIGHTS

- Gamma activity$_{80–150\ Hz}$ was attenuated in the occipital regions during saccades.
- Saccade-related gamma-attenuation was most prominent in the occipital pole.
- Saccade-related gamma-attenuation was noted even during REM sleep.
- Such gamma-attenuation was subsequently followed by gamma-augmentation.
- Longer saccades were associated with more intense gamma-attenuation.

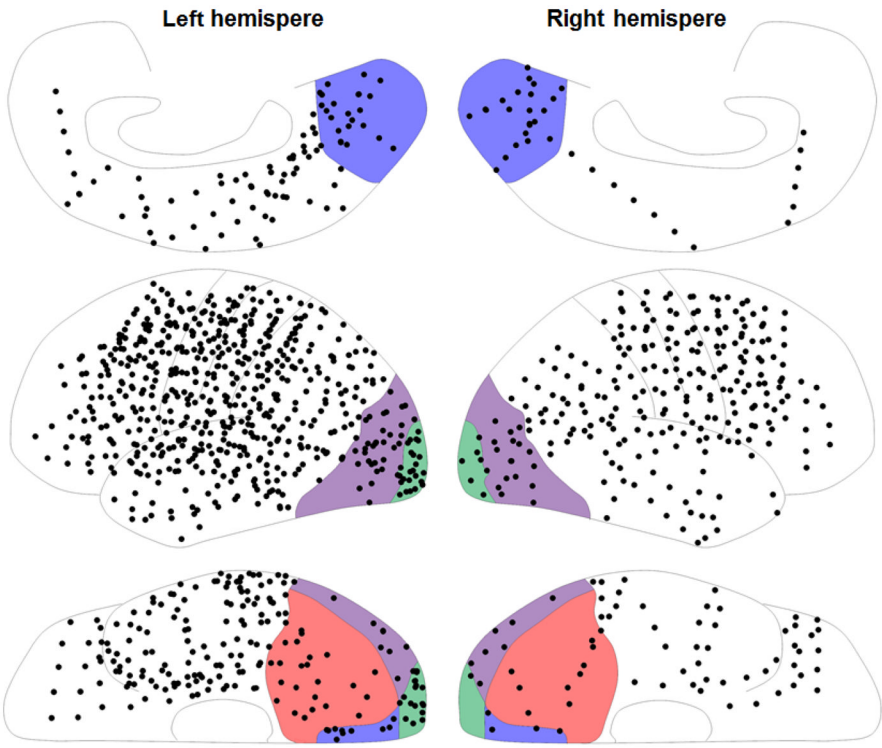

Figure 1. Subdural electrode placement

The locations of subdural electrodes in 10 patients were superimposed on a brain template, as previously performed (Kojima et al., in press; Matsuzaki et al., 2012). The electrodes were implanted on the left hemisphere in seven patients and right hemisphere in the remaining three patients (Table 1). Blue: medial occipital region (medial portion of Brodmann Area (BA) 17/18). Red: inferior occipital region (inferior portion of BA 19/37). Purple: lateral occipital region (lateral portion of BA 19/37). Green: polar occipital region (polar portion of BA 17/18).

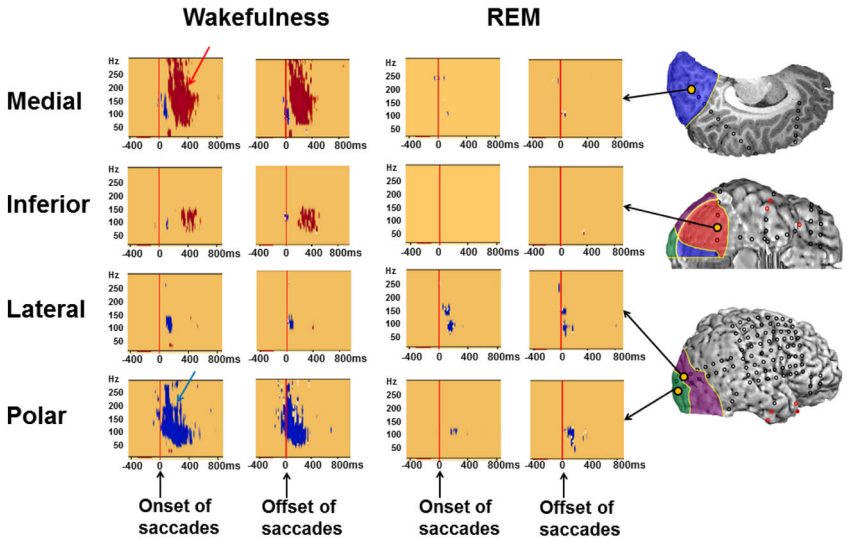

Figure 2. Measurement of saccade-related modulations of ECoG amplitudes

Presented are the results of time-frequency analyses of four electrode sites in Patient #6, who had 51 saccade events marked during wakefulness and 48 during REM sleep. At the onset of saccades during wakefulness, significant gamma-attenuation (denoted by blue color) involved the left polar occipital site and subsequently involved the lateral, medial and inferior occipital sites. Gamma-attenuation in the polar occipital site was lingering and lasted after the saccade offset. Gamma-attenuation in the medial and inferior occipital sites was followed by gamma-augmentation (denoted by red color). At the onset of saccades during REM sleep, significant gamma-attenuation was noted in the polar and lateral occipital sites. No subsequent gamma-augmentation was noted in any of the four sites. The brain surface image shows the locations of subdural electrodes. Blue-shaded area: medial occipital region. Red-shaded area: inferior occipital region. Purple-shaded area: lateral occipital region. Green-shaded area: polar occipital region. Red electrodes: seizure-onset zones. Electrodes with oblique lines: sites excluded from analysis, due to the presence of constant artifacts. The reference period: 300 to 100 ms prior to the saccade onset, and 385 to 185 ms prior to the saccade offset (the mean saccade duration was taken into consideration).

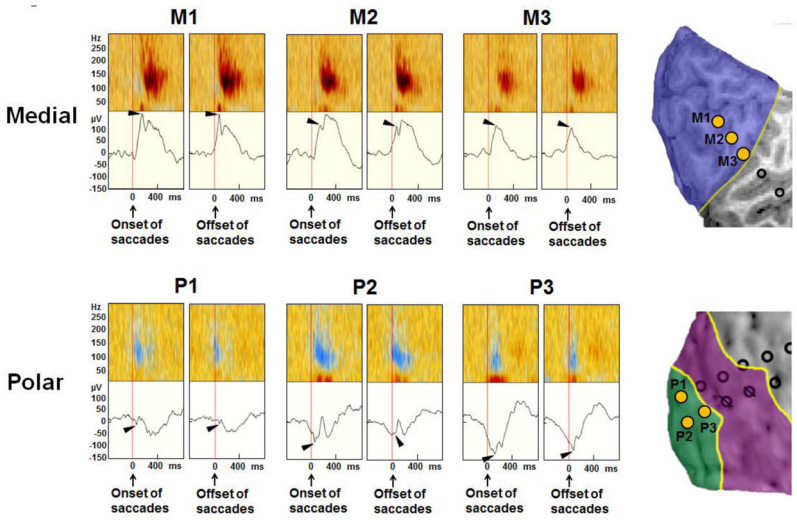

Figure 3. Saccade-related gamma-modulations and concurrent event-related potentials (ERPs)

The medial occipital sites (M1, M2, and M3) showed prominent saccade-related gamma-augmentation (red blobs involving 80–150 Hz) on time-frequency plots; the initial peaks of concurrent ERPs (arrowheads) had a positive polarity, and such ERPs were reflected by brief amplitude augmentation of slow-frequency band on time-frequency plots (red blobs involving <30 Hz). The polar occipital sites (P1, P2, and P3) showed prominent saccade-related gamma-attenuation (blue blobs involving 80–150 Hz); the initial peaks of concurrent ERPs had a negative polarity.

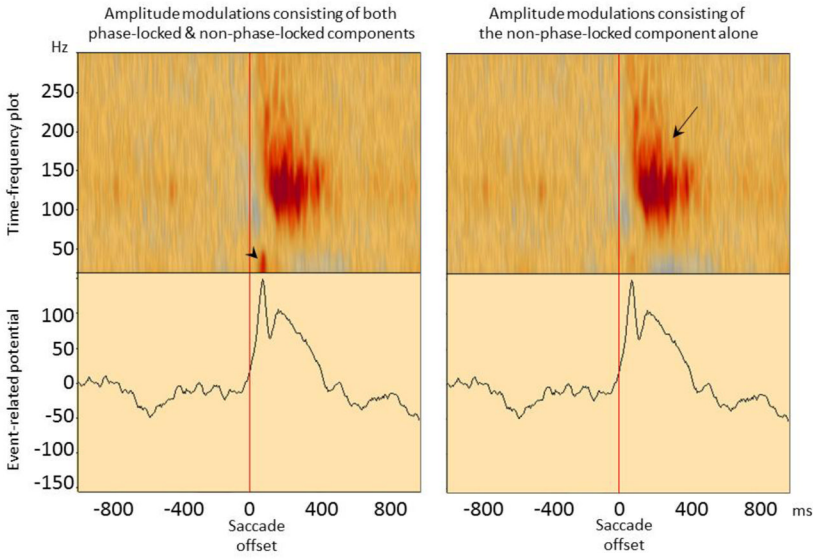

Figure 4. Amplitude modulations consisting of both phase-locked and non-phase-locked components in a medial occipital site

The time-frequency plot on the left side presents the overall amplitude modulations including both phase-locked and non-phase-locked components. The time-frequency plot on the right side presents amplitude modulations only including the non-phase-locked component, by removing the averaged signal (also known as event-related potential) from the single trial time series (Fukuda et al., 2008). Early and brief amplitude augmentation at low frequency band (arrowhead) was considered to be primarily phase-locked to the saccade offset, while gamma augmentation at 80–150 Hz (arrow) was primarily non-phase-locked.

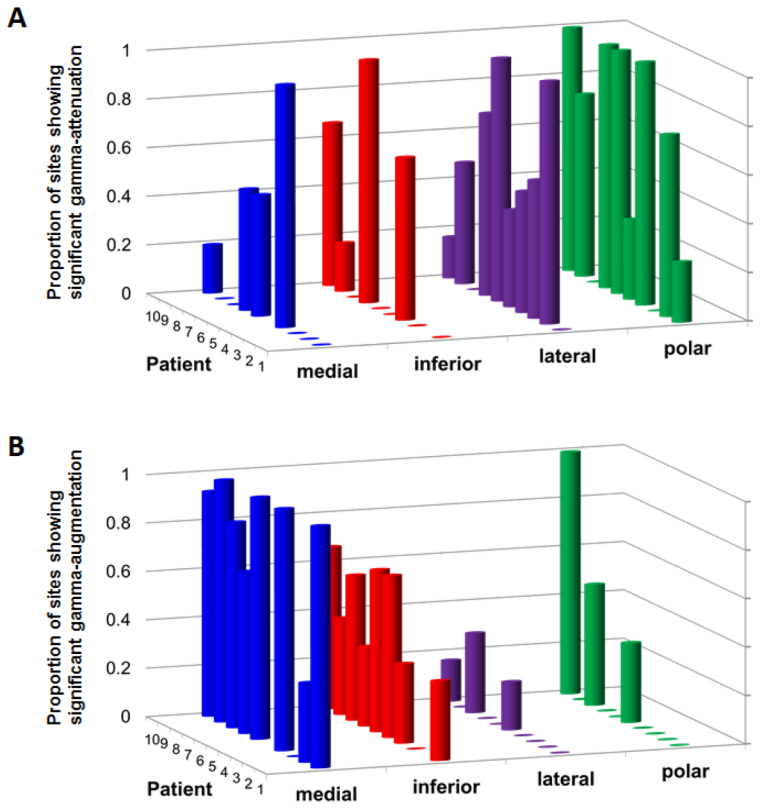

Figure 5. Spatial profiles of saccade-related gamma-modulations

(A) During wakefulness, significant saccade-related gamma-attenuation spanning at least 20-Hz in width (within 80–150 Hz range) and at least 20-msec in duration was noted in 21.3% of medial (95% confidence interval [95%CI]: 11.8 to 35.1%), 26.7% of inferior (95% CI: 14.0 to 44.7%), 38.0% of lateral (95%CI: 25.0 to 53.2%), and 64.5% of polar occipital sites (95% CI: 46.9 to 79.0%). The above observation indicates that the proportions of the polar and lateral occipital sites showing significant gamma-attenuation were greater than those of the medial and inferior occipital sites. (B) Likewise, significant saccade-related gamma-augmentation spanning at least 20-Hz in width and at least 20-msec in duration was noted in 83.0% of medial (95% CI: 69.6 to 91.4%), 46.7% of inferior (95% CI: 30.2 to 63.9%), 11.9% of lateral (95% CI: 4.7 to 25.5%), and 9.7% of polar occipital sites (95% CI: 2.6 to 25.7%).

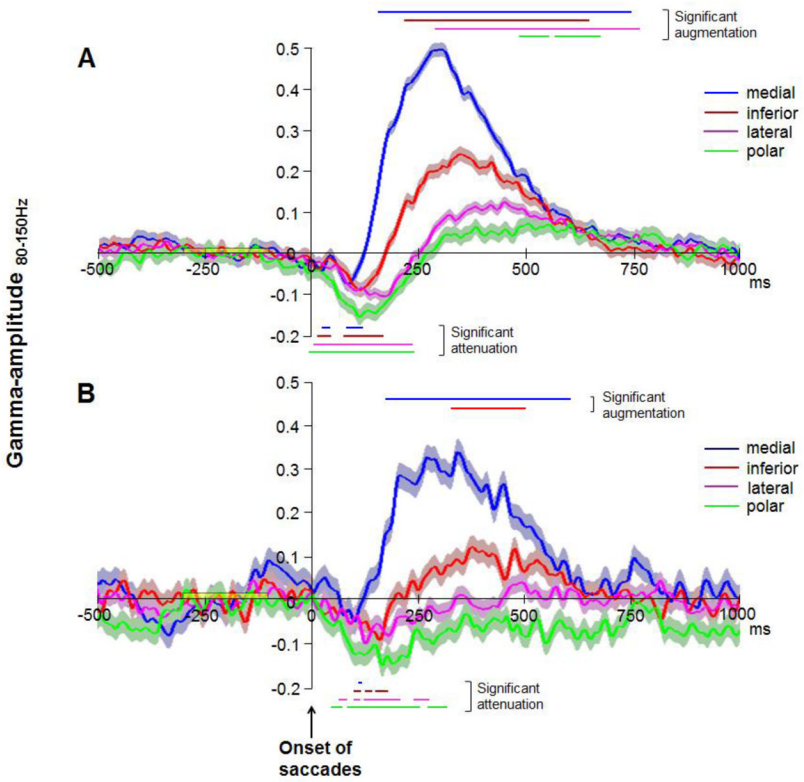

Figure 6. Temporal profiles of saccade-related gamma-modulations

(A) The grand average of gamma-amplitudes$_{80–150Hz}$ across all electrode sites in each occipital region during wakefulness is traced relative to the saccade onset. In summary, gamma-attenuation in the polar and lateral occipital regions began at the saccade onset and lingered even after the saccade offset, whereas that in the medial and inferior occipital regions lasted shorter. Gamma-augmentation sequentially involved the medial, inferior, lateral and polar occipital regions. Standard error is indicated by shading around the trace. (B) Presented is the grand average trace of gamma-amplitudes$_{80–150Hz}$ across electrodes in each occipital region during REM sleep. Gamma-attenuation following the onset of saccades initially involved the polar occipital region and subsequently involved the remaining occipital regions. Gamma-augmentation was less intense during REM sleep compared to wakefulness; no significant gamma-augmentation, at the regional level, was noted in the polar or lateral occipital region.

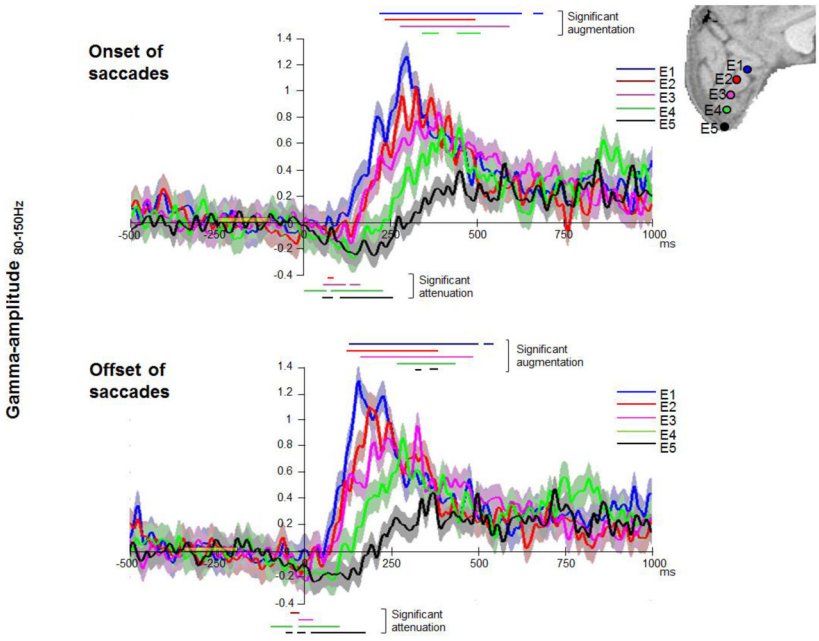

Figure 7. Gradient in saccade-related gamma-modulations across neighboring occipital sites

Gamma-amplitudes$_{80–150Hz}$ during wakefulness at five medial occipital sites in patient #7 are traced relative to the saccade onset. Electrode 5 (black trace), located posteriorly and close to the polar occipital region, showed intense gamma-attenuation, which was followed by the smallest gamma-augmentation among the five sites. Conversely, anterior-located electrode 1 showed no gamma-attenuation during saccades but subsequently showed the largest and earliest gamma-augmentation among the five sites (blue trace). Standard error is indicated by shading around the trace.

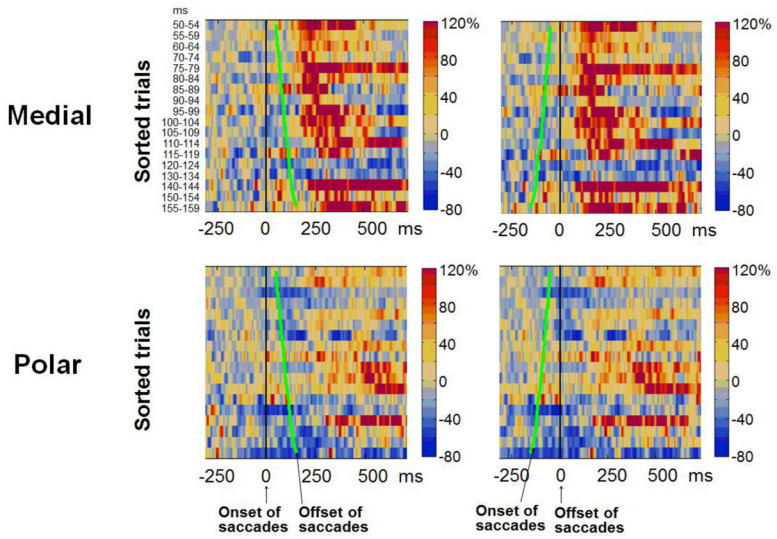

Figure 8. Trial-by-trial time-frequency analysis

Presented are the temporal changes of gamma-amplitudes$_{80–150Hz}$ during wakefulness in the medial and polar sites of patient #6. The x-axis represents time, while the y-axis represents trials sorted according to the duration of saccade. Each row shows gamma-amplitudes$_{80–150Hz}$ (averaged across trials every 5 ms width of saccade duration) as a function of time. Gamma-augmentation (red) in the medial occipital site was better time-locked to the offset of saccades. Gamma-attenuation (blue) in the polar occipital site lingered even after the saccade offsets in many trials.

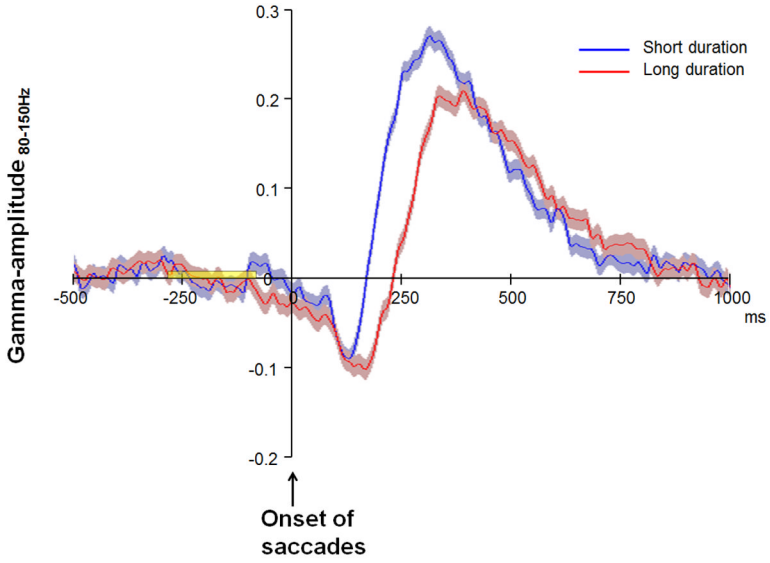

Figure 9. Relationship between the saccade duration and saccade-related gamma-attenuation

Presented are gamma-amplitudes$_{80–150Hz}$ during wakefulness averaged across all 150 occipital sites in trials of which saccade durations were shorter (blue trace) or longer (red trace) than the median of each patient. Standard error is indicated by shading around the trace. Each saccade had an inter-saccade interval of >1000 ms. We determined whether the least square (LS) means of minimum gamma-amplitude$_{80–150Hz}$ as well as that of peak latency of minimum gamma-amplitude$_{80–150Hz}$ differed between trials with shorter and longer durations. Thereby, a mixed-model ANOVA was employed on 150 occipital sites with the saccade-duration group treated as a fixed effect and patients treated as a random effect. The saccade duration (‘shorter’ versus ‘longer’) had a significant effect on the LS means of minimum gamma-amplitude$_{80–150Hz}$ (df: 1; F=10.6; p=0.001), but no effect on the LS means of peak latency of minimum gamma-amplitude$_{80–150Hz}$ (df: 1; F=2.6; p=0.15). In short, the trials with longer saccade durations were associated with more intense perisaccadic gamma-attenuation.

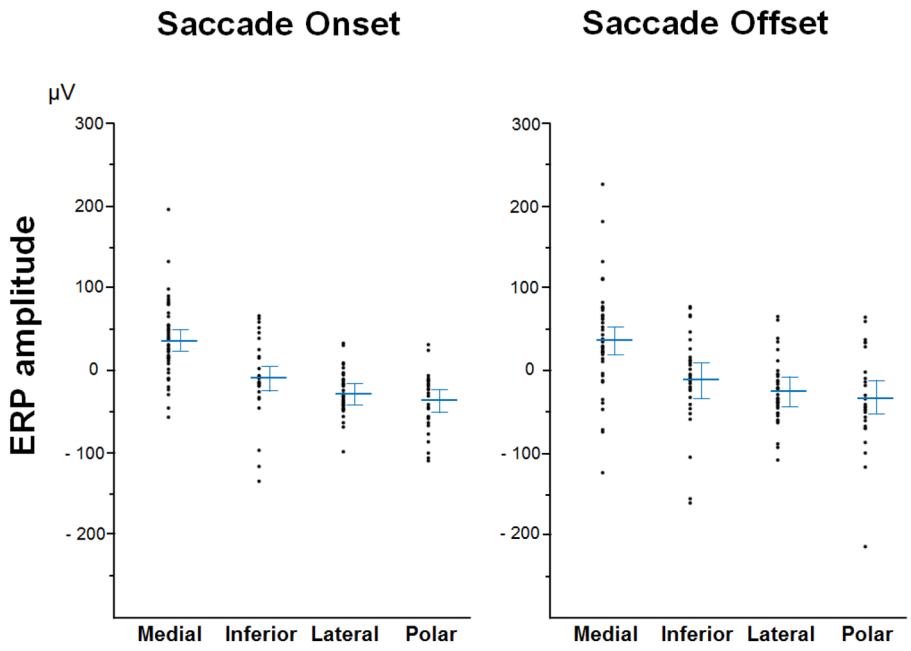

Figure 10. The baseline-to-peak voltage of the first peak in peri-saccadic ERP

Left: the results derived from ERPs time-locked to the saccade onset. Right: the results derived from those time-locked to the saccade offset. Each dot represents the baseline-to-peak voltage of the first ERP peak in each occipital site. The means and standard error bars are shown.

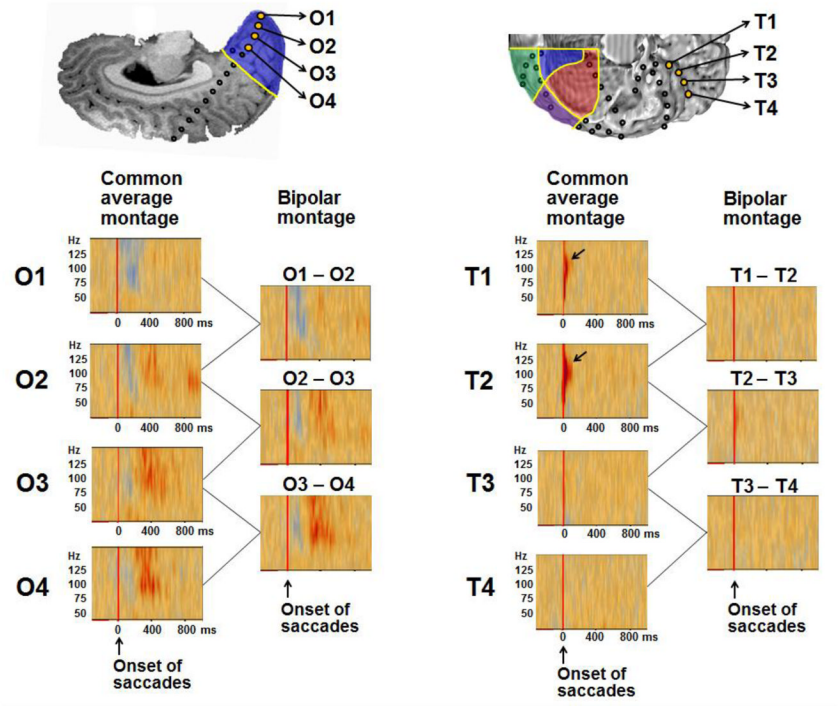

Figure 11. Perisaccadic gamma-modulations on common average and bipolar montage

Left: Occipital gamma-modulations of cortical origin are well appreciated on common average and bipolar montage. Right: Ocular EMG-elicited gamma-augmentations are noted at T1 and T2 in the anterior temporal regions at the saccade onset (arrows). Bipolar montage effectively eliminated such spurious gamma-augmentation (Jerbi et al., 2009a; Nagasawa et al., 2011).

Neuroimage. Author manuscript; available in PMC 2014 December 01.

Table 1

Clinical profiles of patients

Patient	Gender	Age (years)	VCI	Handedness	Sampled hemisphere	Seizure onset zone	Antiepileptic medications
1	Female	5	80	Left	Left	Frontal-temporal	LEV, PHT, OXC, TPM
2	Male	5	77	Left	Left	Frontal-parietal	LEV, LTG
3	Female	7	75	Right	Left	Frontal	OXC, ZNS
4	Female	9	100	Right	Left	Frontal	VGB, CBZ VPA
5	Male	10	71	Right	Right	Temporal	OXC
6	Female	11	114	Right	Right	Temporal	LEV, OXC
7	Female	14	124	Right	Left	Frontal	LEV, OXC, LCM
8	Female	16	121	Right	Left	Occipital	OXC, LEV
9	Male	17	110	Right	Left	Temporal	OXC
10	Female	17	100	Right	Right	Parietal-occipital	LEV, OXC

VCI: Verbal Comprehension Index, LEV: Levetiracetam, PHT: Phenytoin, OXE: Oxcarbazepine, TPM: Topiramate, LTG: Lamotrigine, ZNS: Zonisamide, VGB: Vigabatrin, CBZ: Carbamazepine, VPA: Valproic acid, LCM: Lacosamide

Table 2

Number of analyzed saccade events and sampled sites

Patient	Number of analyzed saccades		Number of implanted occipital electrodes				
	WK	REM	Medial	Inferior	Lateral	Polar	Total
1	65	29	2	3	3	4	12
2	59	43	3	0	2	4	9
3	67	22	1	2	7	2	12
4	34	13	2	3	2	2	9
5	68	36	0	3	5	3	11
6	51	48	4	3	2	3	12
7	49	9	6	3	4	6	19
8	73	12	13	5	9	2	29
9	62	37	1	5	2	4	12
10	63	16	15	3	6	1	25
total	591	265	47	30	42	31	150

WK: wakefulness, REM: rapid eye movement sleep